View metadata, citation and similar papers at core.ac.uk

brought to you by CORE

provided by University of Kentucky

University of Kentucky
UKnowledge

Biosystems and Agricultural Engineering Faculty Publications

Biosystems and Agricultural Engineering

9-2004

Vertical Wall Loads in a Model Grain Bin with Non-Axial Internal Inserts

Marek Molenda
Polish Academy of Sciences, Poland

Michael D. Montross
University of Kentucky, michael.montross@uky.edu

Jozef Horabik
Polish Academy of Sciences, Poland

Sidney A. Thompson
University of Georgia

Right click to open a feedback form in a new tab to let us know how this document benefits you.

Follow this and additional works at: https://uknowledge.uky.edu/bae_facpub

Part of the Agriculture Commons, and the Bioresource and Agricultural Engineering Commons

Repository Citation

Molenda, Marek; Montross, Michael D.; Horabik, Jozef; and Thompson, Sidney A., "Vertical Wall Loads in a Model Grain Bin with Non-Axial Internal Inserts" (2004). *Biosystems and Agricultural Engineering Faculty Publications*. 93.
https://uknowledge.uky.edu/bae_facpub/93

This Article is brought to you for free and open access by the Biosystems and Agricultural Engineering at UKnowledge. It has been accepted for inclusion in Biosystems and Agricultural Engineering Faculty Publications by an authorized administrator of UKnowledge. For more information, please contact UKnowledge@lsv.uky.edu.

Vertical Wall Loads in a Model Grain Bin with Non-Axial Internal Inserts

Notes/Citation Information
Published in *Transactions of the ASAE*, v. 47, issue 5, p. 1681-1688.

© 2004 American Society of Agricultural Engineers

The copyright holder has granted the permission for posting the article here.

Digital Object Identifier (DOI)
https://doi.org/10.13031/2013.17610

This article is available at UKnowledge: https://uknowledge.uky.edu/bae_facpub/93

VERTICAL WALL LOADS IN A MODEL GRAIN BIN WITH NON-AXIAL INTERNAL INSERTS

M. Molenda, M. D. Montross, J. Horabik, S. A. Thompson

ABSTRACT. *A study was conducted to estimate the degree of load asymmetry in a bin with non−axial internal inserts. Internal inserts in the form of an annulus segment were attached to the wall, and their influence on vertical wall loads during centric filling and discharge in a model bin were measured. Wall and floor loads were measured in a corrugated−wall model grain bin with a diameter of 2.44 m and a height of 7.3 m filled with soft red winter wheat to a depth of 6.7 m (height−to−diameter ratio of 2.75). Tests were conducted with inserts that extended circumferentially 30˚, 60˚, or 90˚ around the bin, having a width of 7.6, 15, or 23 cm and attached to the bin wall at height−to−diameter (H/D) ratios of 0.31, 0.62, or 0.95. These inserts represented between 1% and 8.6% of the bin floor area. The results showed that with centric filling, considerable asymmetry of static wall loads occurred. The asymmetric loading was caused by the horizontal component of the velocity of the grain stream filling the bin, produced by the drag conveyor. This loading created wall moments in the bin of approximately 3 kN−m. The wall moments generated by imperfect centric filling varied depending on the angular position of the inserts. For a 23 cm wide, 90˚ insert, which was the worst observed situation, the wall moment was approximately 5 kN−m. The onset of symmetric discharge resulted in an increase in vertical wall load and a decrease in the wall moment. A change in flow pattern from mass flow to funnel flow, as well as the influence of the insert, was clearly shown by the change in wall moment with discharge time.*

Keywords. *Asymmetry, Obstruction, Wheat.*

Most of the current grain bin design standards are based on Janssens's equation (1895), which assumes a uniform stress state around and across the cross−section of a bin. However, in practice some unloading and loading conditions can create a non−uniform stress state within the bin. These non−uniform stress states in grain bins are believed to be the cause of many structural failures in grain bins. In 1919, Ketchum recommended that designers locate discharge gates only at or near the bin center to minimize non−uniform stresses. According to Bucklin et al. (1990), the majority of bin design methods assume that wall failure in bins is caused by circumferential bending moments originating from a non−uniform distribution of lateral stresses on the bin wall. However, bin wall failures were observed in practice (Ravenet, 1981) as well as experimentally (Bucklin et al., 1990) to be caused by meridional bending moments resulting from non−uniform vertical forces on the bin wall. Timoshenko (1910) derived an equation for calculating the critical buckling stress for thin−walled cylinders under axial compression. However, the theoretical buckling stress is never reached in practice because of geometric imperfections of the fabricated cylinder. Empty thin−walled cylindrical shells typically buckle at stress levels between 10% and 30% of theoretical values (Bucklin et al., 1990).

Wilms (1994) outlined a number of areas of unsolved problems in silo design. Two areas where research was lacking were the determination of boundary lines between flowing and stagnant grain and the prediction of the effect that internal obstructions have on flow alteration. These internal obstructions can cause structural problems by creating a non−uniform pressure distribution within a bin. Current silo standards do not contain design rules for analyzing such loads. Carson (2000) regarded bending of the circular bin wall caused by eccentric discharge as one of the most common causes of structural problems. If the resulting flow channel intersects the silo wall, then non−uniform pressures develop around the circumference of the silo, leading to horizontal and vertical bending moments. Support beams, inverted cones, blend tubes, and other types of internal structures can all impose large concentrated loads and/or non−symmetric pressures on the silo wall. In these cases, unsymmetrical pressures are unavoidable because of the non−axial location of the inclusion. These induce bending moments in the wall and can initiate buckling of the wall in a steel silo.

According to Sundaresan (2001), establishing and maintaining flow symmetry is one of the unsolved challenges involved in the handling of cohesionless particles. The author suggested that even during centric discharge unstable conditions could occur that result in asymmetric discharge

Article was submitted for review in September 2003; approved for publication by the Structures & Environment Division of ASAE in July 2004. Presented at the 2002 ASAE Annual Meeting as Paper No. 024031.

The authors are **Marek Molenda, ASAE Member Engineer,** Assistant Professor, and **Jozef Horabik, ASAE Member Engineer,** Professor, Institute of Agrophysics, Polish Academy of Sciences, Lublin, Poland; and **Michael David Montross, ASAE Member Engineer,** Assistant Professor, Department of Biosystems and Agricultural Engineering, University of Kentucky, Lexington, Kentucky; and **Sidney A Thompson, ASAE Member Engineer,** Professor, Department of Biological and Agricultural Engineering, University of Georgia, Athens, Georgia. **Corresponding author:** M. D. Montross, Department of Biosystems and Agricultural Engineering, 128 Barnhart Building, University of Kentucky, Lexington, KY 40546−0276; phone: 859−257−3000 ext. 106; fax: 859−257−5671; e−mail: montross@bae.uky.edu.

 © 2004 American Society of Agricultural Engineers ISSN 0001−2351

patterns, with the imperfect discharge providing the necessary stimulus to cause destabilization. Rotter (1998) observed in a review of shell structure design rules that axial symmetry of stresses was often assumed. Rotter suggested that a typical cause of bin failure was a result of local unsymmetrical normal pressures on the bin wall, with the primary cause of these pressures a result of unsymmetrical mass flow. Extensive work on the effect of local high stresses was needed to provide an explanation of these phenomena.

Australian Standard AS 3774 (1996) states that unsymmetrical internal features restrict flow and are one of the four main sources of eccentric flow patterns. It also recommended using flow conditions to determine the forces on internal structural elements located within the stored solid. For internal structural elements located below the transition point between mass flow and funnel flow, the forces can be determined using initial pressures. However, Tsunakawa and Aoki (1975) showed that the vertical force exerted on an object in the bin could not be estimated from the vertical stress predicted by Janssen's equation. Eurocode 1 (CEN, 1996) and ISO 11697 (ISO, 1995) do not address the influence of inserts on bin loads. No standard addresses the degree of asymmetry caused by internal elements within a bin.

In practice, small inclusions act similarly to structural imperfections and can initiate buckling, while larger flow obstacles can significantly alter the stress distributions. A mass of static agglomerated grain bound to part of the wall can act as a non−symmetric inclusion that could cause buckling failure of the bin wall. No analytical solution or numerical simulation method is currently available to estimate loads caused by an eccentric inclusion in a bin.

The objective of this study was to estimate the degree of load asymmetry in a bin with an insert in the form of an annulus segment attached to the wall. Values of wall overturning moments were determined with respect to variation in insert width, circumferential extent, and height of the insert above the bin floor.

EQUIPMENT, PROCEDURE, AND MATERIAL

All tests were performed in a model grain bin 2.44 m in diameter with a height of 7.3 m. The walls of the bin were made of corrugated galvanized steel. The horizontal corrugations had a pitch and depth of 67.5 and 13 mm, respectively. The model bin was equipped with a flat floor. The cylindrical wall of the bin and the flat floor were each supported independently to isolate the wall and floor loads. The wall and floor of the model grain bin were each supported by three load cells spaced at an angle of 120° around the circumference of the bin. The bin was centrally filled at a flow rate of approximately 250 kg/min using a horizontal conveyor equipped with a discharge spout. After filling, the grain was allowed to equilibrate during a detention period of 0.5 h. The wheat was then discharged from the bin through an 89 mm diameter discharge orifice located in the center of the bin, which produced a sliding velocity of 3.2 m/h along the bin wall during mass flow. The wall and floor loads during loading, detention, and discharge were measured at 1 min intervals until discharge was completed. To observe the dynamic response of the loads at the start of grain discharge, loads were measured at 0.1 s time intervals prior to opening the unloading orifice and for 1 min after the start of discharge. The loads were measured with an accuracy of ±100 N. All tests were conducted using centric filling and centric discharge.

To produce asymmetry of loads, horizontal inserts were attached to the bin wall. Tests were conducted using inserts in the shape of a portion of an annulus. The inserts were constructed from 19 mm thick plywood and extended circumferentially around the bin in arc lengths of 30°, 60°, or 90°. The inserts had widths of 7.6, 15, or 23 cm and were attached to the bin wall at height−to−diameter (H/D) ratios of 0.31, 0.62, or 0.95 above the floor of the bin. The percent floor area covered by the inserts varied between 1.0% and 8.6%. The widths and location of the inserts were chosen based on experiments performed by Kim (cited by Turitzin, 1963). Kim applied wooden rings inside a bin to change the flow pattern of grain. He determined that rings 15.2 cm wide were effective in altering the flow pattern within the bin. The rings prevented sliding of grain along the bin wall, which resulted in the formation of funnel flow within the bin. This prevented an increase in the dynamic pressure on the bin walls. However, smaller rings 8.2 cm wide did not produce funnel flow. Kim proposed that the smaller rings did not project into the flowing grain far enough to alter the flow pattern.

Kim suggested that there was a qualitative difference in the interaction between the grain and the wooden rings for the two reported cases. This information was utilized to determine the depth of the inserts applied in this project. In earlier experiments in this bin (Molenda et al., 2001), for the first several seconds after initiation of discharge, grain was observed to move along the bin wall down to a grain height of 0.80 m (H/D ratio of 0.32) above the bin floor. During the next 30 s, the level at which no grain movement was observed along the bin wall increased to approximately 1.8 m (H/D ratio of 0.74) and remained constant until the flow pattern changed from mass flow to funnel flow. Mass flow was observed to cease after the grain level reached an H/D ratio between 1.37 and 1.71. Based on the flow conditions that existed within the model test bin, the inserts were attached to the bin wall at the following H/D ratios: 0.31 (0.86 m from the floor), 0.62 (1.51 m), and 0.95 (2.31m). These locations would place the inserts in the dead zone (the area along the wall in the bottom of the bin with no flow), between the dead zone and mass flow, and in the mass flow region, respectively. The locations of the insert, the discharge orifice, and the floor and wall load cells are shown in figure 1.

A total of 33 tests were performed in which inserts were randomly attached to the wall at various heights, angular extents, and widths. Four preliminary tests were performed with no inserts to establish conditions of equilibrium between the grain and bin wall. In addition, to observe the degree of wear−in effects, the 12th, 23rd, and 33rd tests were performed with no inserts. In general, inserts were attached to the section of wall lying in the ($+x$, $-y$) quadrant of the bin coordinate system. Three tests were performed with 90° inserts attached to the bin walls at an H/D of 0.62 in the ($+x$, $+y$) quadrant of the bin coordinate system to estimate the influence of imperfect centric filling on load asymmetry. Each experimental condition was performed without replication. Previous experiments allowed for the estimation of run−to−run variability as well as its sources. Tests were repeated if outlying results were obtained.

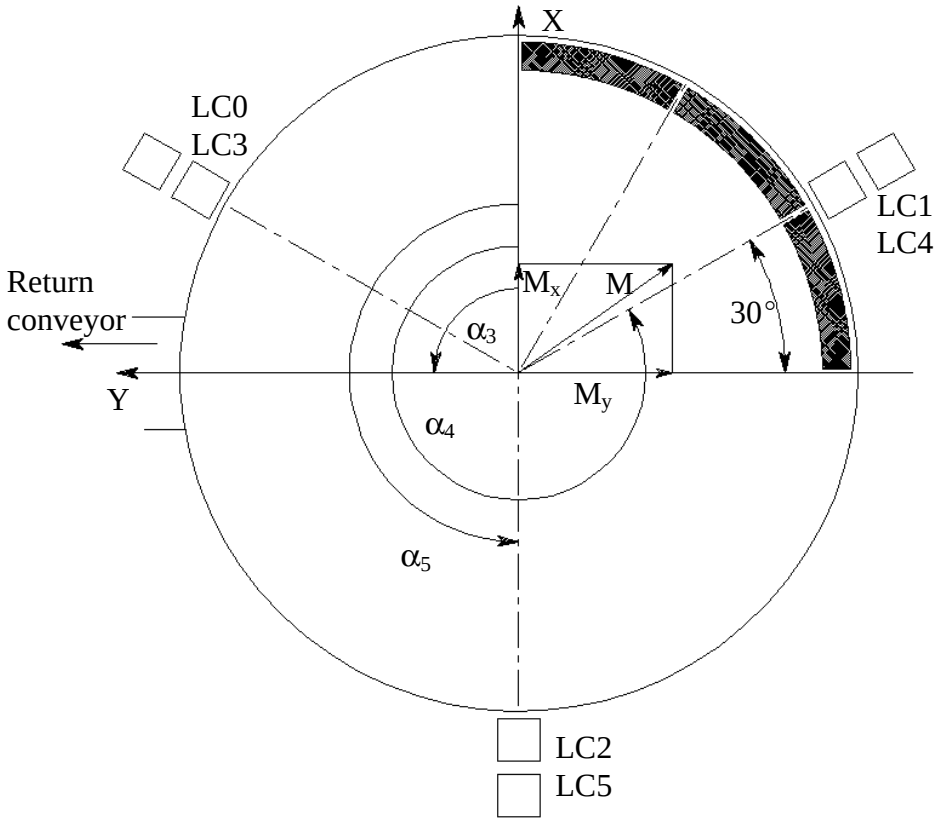

Figure 1. Location of load cells (LC0 through LC5) and inserts in the model grain bin (top view).

Tests were conducted using soft red winter wheat with an uncompacted bulk density of 760 kg/m^3 and moisture content of 12.5% (w.b.). Friction tests were performed to determine the angle of internal friction after the 1st, 10th, 20th, and 30th tests, and values of 26° ±0.6°, 25.5° ±0.0°, 24.4° ±0.4°, and 24.0° ±0.3° were found, respectively (Molenda et al., 2002). No significant value of cohesion was found, and the material was treated as free−flowing grain. The observed decrease in the angle of internal friction was attributed to damage of the grain caused by repeated handling and contributed to the variation in the measured bin loads.

The presence of an insert prevented grain movement along the bin wall directly above the insert. The zones of stagnant grain for the 7.6, 15, and 23 cm wide inserts were 30, 70, and 100 cm, respectively, measured above the midpoint of the insert.

Analysis of Bin Wall Data

Total vertical floor loads (F_{vl}) and total vertical wall loads (W_{vl}) were calculated using the following equations:

$$F_{vl} = F_o + F_1 + F_2 \quad (1)$$

$$W_{vl} = F_3 + F_4 + F_5 \quad (2)$$

where

F_{vl} = vertical forces carried by the floor (floor load cells 0, 1, and 2) (N)

W_{vl} = vertical forces carried by the wall (wall load cells 3, 4, and 5) (N).

The longitudinal bending wall moments in the bin about each of the major axes were calculated using the following equations:

$$M_x = R\left(F_3 \sin\alpha_3 + F_4 \sin\alpha_4 + F_5 \sin\alpha_5\right) \quad (3)$$

$$M_y = -R\left(F_3 \cos\alpha_3 + F_4 \cos\alpha_4 + F_5 \cos\alpha_5\right) \quad (4)$$

where

M_x = moment about the x axis of the bin (N m)

M_y = moment about the y axis of the bin (N m)

α_i = angular coordinates of load cell i with respect to the x axis (°)

R = distance of the load cell from the vertical axis of the bin (m).

Values of the resultant moment (M) were calculated using:

$$[M] = \left[M^2{}_x + M^2{}_y\right]^{1/2} \quad (5)$$

Results

Symmetric Load Conditions

Changes in the frictional characteristics of the grain−wall interface and the resulting change in the angle of internal friction resulted in a decrease in the vertical wall load (VWL) during the testing period. Figure 2 shows the ratio of the vertical wall load to total grain load contained in the bin (VWL/TGL) determined at the start of discharge and after the 2nd, 13th, and 23rd tests. The ratios found for static conditions (at the end of detention period) were 59.7%, 55.4%, and 52.6%, respectively. After 60 s of discharge, the corresponding values were 64.1%, 61.2%, and 59.6%. A change in the basic response of the VWL/TGL against time relationship was also observed. The 2nd test had a smooth, asymptotic behavior after opening of the discharge gate,

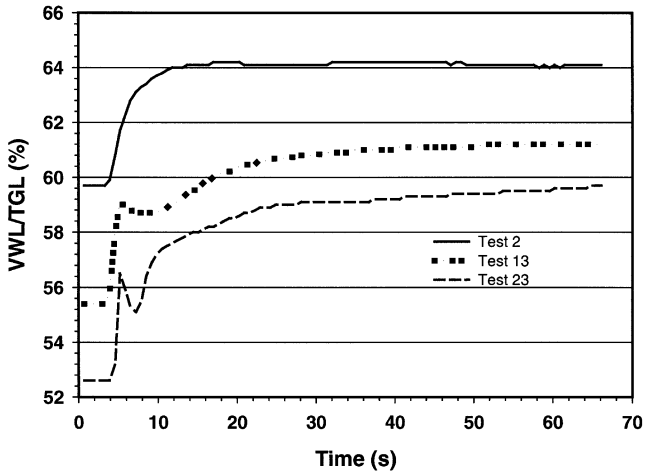

Figure 2. Ratio of vertical wall load to total grain load (VWL/TGL) at the onset of discharge for the 2nd, 13th, and 23rd tests.

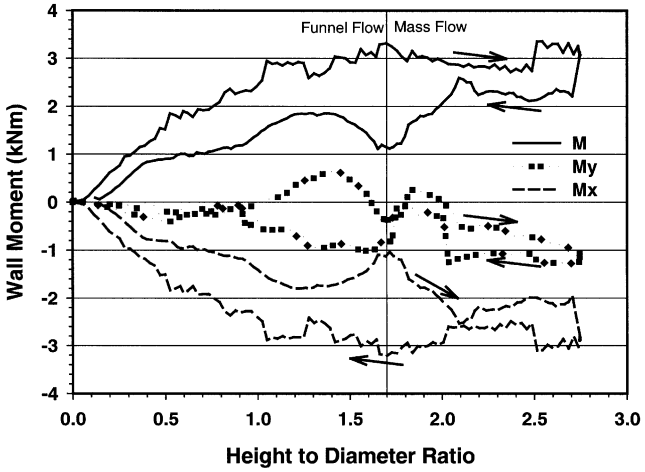

Figure 3. Wall moments produced during centric filling (arrows pointing to the right) and discharge (arrows pointing to the left) of the model bin with no insert on the wall.

while the 13th and 23rd tests had a load spike immediately after opening the discharge gate, followed by an increase up to the maximum wall load. This kind of behavior is a transient response of the elastic structure to a sudden increase in load. None of the currently recommended design procedures predict this reaction of the structure because the theoretical approaches involved do not take into consideration dilation of grain at the start of discharge.

During centric filling and centric discharge of a bin, a perfectly symmetric stress distribution is normally assumed to occur in which constant frictional conditions are assumed to act on the bin wall. For these conditions, the wall moments acting on the bin should theoretically be zero. However, during these experiments, moments were produced in the bin, even during centric unloading and loading, because of imperfections in the bin. Figure 3 shows the wall moments during centric filling and discharge for the 2nd test (with no insert). The wall moments observed in this graph constitute the background moments for the tests with inserts. The resultant moment (M) increased quickly during filling up to a fill height of an H/D ratio of approximately 1. Above this H/D ratio, the moments remained in a narrow range around 3 kN−m, with a maximum observed value of 3.3 kN−m. The components M_x and M_y of the resultant moment (M) are shown in figure 3. The M_y component reached a maximum of 1.2 kN−m during filling and fluctuated to a lesser degree than the M_x component of the wall moment. The maximum value of M_x was found to be 3.2 kN−m for an H/D of approximately 1.8 during filling of the bin.

The main reason for the observed asymmetry of loads during filling was imperfect centric filling. In the grain handling system, grain is transported overhead by a drag conveyor. As the grain leaves the drag conveyer, it has a horizontal component of velocity. Consequently, the grain falling into the bin does not follow a straight vertical line corresponding to the vertical axis of the bin. This component of velocity was directed along the y axis of the bin and resulted in a larger increase in the M_x component of the wall moment (see fig. 3). As the height of grain in the bin increased, grain was deposited on the mass closer to the axis of the bin, which resulted in a more uniform distribution of pressure across the horizontal cross−section of the bin.

Geometrical inaccuracies in the cylindrical bin wall and/or non−uniformity of the wall friction throughout the bin surface were also thought to contribute to wall load asymmetry. Ramps were visible on the loading curves, which reflected instability of the formed structure because of grain bedding. A rearrangement of portions of the grain in the bin along the cone of repose occurred after some grain was deposited on the surface.

The opening of the centric discharge orifice resulted in an increase in wall load and initiation of mass flow with grain sliding against the bin wall. At the onset of mass flow, a rapid drop occurred in the wall moment about the x axis of the bin, with this value decreasing down to approximately 2.3 kN−m. During continued unloading, the wall moment (M_x) slowly continued to increase to 2.6 kN−m at an H/D ratio of approximately 2.1. At this point, the moments decreased significantly down to the location where the flow pattern changed from mass flow to funnel flow, and fluctuations in the wall loads and wall moments occurred. After the change in flow pattern, the wall moment increased slightly and then decreased smoothly until the bin was empty.

WALL LOADS WITH INSERTS ATTACHED

Wall Loads Acting on One Load Cell During Loading and Unloading

Figure 4 shows the ratio of the vertical wall load measured by load cell 3 to total grain load (VWL3/TGL) during centric loading and unloading of the bin for two different test conditions. One test was conducted with no insert. The second test included an insert 23 cm wide attached to the bin wall at an H/D ratio of 0.62. The insert spanned a 90˚ arc and was located in the (+x, −y) quadrant of the bin, as shown in the figure. During loading, both loading curves followed a common path up to an H/D level of approximately 0.6 (the location of the insert). During further loading, the VWL3/TGL for the test condition with an insert was higher than the test with no insert. It is believed that the higher vertical loads were caused by overbearing grain, which was supported by the insert. At the end of loading, the VWL3/TGL was determined to be 19.7% for the test with the insert and 18.1% for the test with no insert. Initiation of centric discharge resulted in an increase in the loading ratio of up to 22% for the wall with an insert and 20.3% with no insert. During the entire period of unloading, the VWL3/TGL ratio in the bin with the insert remained higher than the load

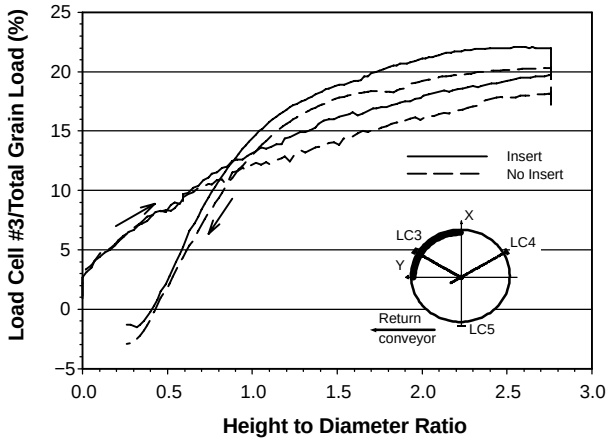

Figure 4. Ratio of load recorded by LC3 to total grain load during filling (arrows pointing to the right) and discharge (arrows pointing to the left) of the model bin with no insert and with a 23 cm, 90˚ insert attached to the wall at H/D = 0.62 in the (+*x*, −*y*) quadrant.

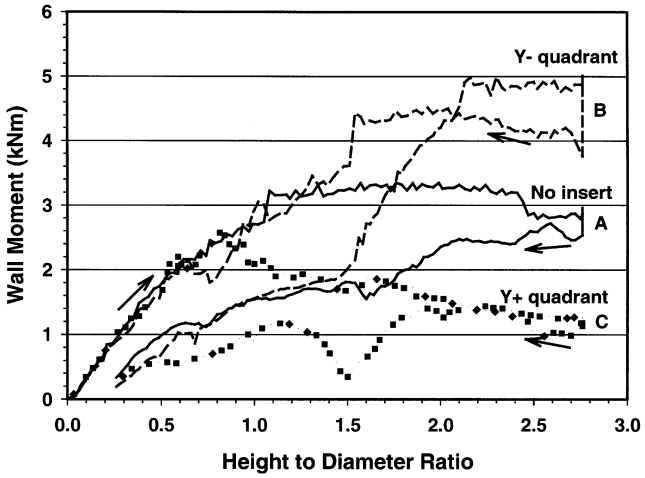

Figure 5. Wall moments produced during filling (arrows pointing to the right) and discharge (arrows pointing to the left) of the bin, with no insert (test A) and with a 90˚, 23 cm wide insert attached to the wall at an H/D ratio of 0.62, located in the (+*x*, +*y*) quadrant of the bin (test B) and in the (+*x*, −*y*) quadrant of the bin (test C).

ratio in the bin with no insert. A smaller magnitude of negative friction force was also recorded by load cell 3 at the end of unloading with the insert. For this test, the grain was assumed to be less compacted under the insert and, therefore, accumulated a smaller amount of elastic energy, which resulted in a smaller elastic reaction.

Static and Dynamic Wall Loads

The ratio of the vertical wall load to total grain load (VWL/TGL, expressed in %) was calculated at the end of filling and after 60 s of discharge for the 23 cm wide insert. Immediately after opening the discharge gate, a large increase in vertical wall load was observed to occur. The ratio of the total wall loads in the dynamic to static condition was expressed as the dynamic−to−static wall load ratio (DSR). Values for VWL/TGL and DSR are presented in table 1. Static VWL/TGL after the detention period were found in the range from 51% (with no insert) to 57% (with a 90˚, 23 cm wide insert located at H/D ratios of 0.31 and 0.62). After 60 s of discharge, values of VWL/TGL were found in the range between 60% for no insert and up to 64% when an insert, was used. Both static and dynamic values of VWL/TGL were higher with inserts that extended over a greater arc within the bin. The location of the insert (H/D ratio) did not appear to have a significant effect on the VWL/TGL or the DSR. The DSR values were found to vary over a range from 1.11 to 1.16, without a clear relationship to describe the effect that either the extent or the height of the insert had on vertical wall loads.

Table 1. Percent of the total grain load supported by the bin wall and dynamic−to−static load ratios (DSR) for four radial extents and three heights of attachment of the insert.

		VWL/TGL (%)[a]		
H/D	Extent (°)	End of Filling	After 60 s of Discharge	DSR
0.31	0	53	60	1.13
	30	54	60	1.12
	60	55	61	1.11
	90	57	64	1.13
0.62	0	53	60	1.12
	30	53	61	1.15
	60	55	63	1.15
	90	57	64	1.13
0.95	0	51	60	1.16
	30	53	61	1.16
	60	54	62	1.14
	90	56	64	1.15

[a] The percent of the total grain load in the bin was calculated at the end of filling and again after 60 s of discharge.

WALL MOMENTS DURING LOADING AND UNLOADING

Wall Moments for Different Circumferential Location of Insert

Figure 5 shows the resultant wall moments for three different experimental conditions: test A, with no insert, and tests B and C, in which a 23 cm wide insert spanning a 90˚ arc was attached to the bin wall at an H/D ratio of 0.62. For all three tests, the resultant wall moments followed a similar path during filling until the grain level reached the insert. From this graph, it is apparent that the location of the insert with respect to the *y* axis had an effect on the resultant wall moments in the bin. During test B, the insert was located in the (+*x*, +*y*) quadrant of the bin (see fig. 1). When the insert was located on the positive side of the *y* axis, the resultant wall moment increased in a manner similar to the test with no insert. During test C, the insert was located in the (+*x*, −*y*) quadrant of the bin. When the insert was located on the negative side of the *y* axis, the wall moment was lower relative to tests A and B.

For test A, a maximum wall moment of 3.3 kN−m was found. The wall moments associated with test A, in which no insert was used, are background moments caused by off−center filling and geometric imperfections in the bin. For test B, the resultant wall moment was higher than those of test A, indicating that the moments created by the insert acted in the same direction as those of the background moment, and the insert amplified the moments within the bin. A maximum wall moment of 5 kN−m was observed for test B at the end of filling. For test C, a maximum moment of 2.4 kN−m was measured during filling, not at the end of filling, but rather at an H/D ratio of approximately 0.9. For test C, the wall moments at the end of filling were approximately 1.3 kN−m,

well below the background moments normally associated with the imperfections in the bin. This indicates that the moments due to the inserts acted in the opposite direction of those associated with the bin imperfections.

After initiation of discharge, a sharp decrease in the wall moment was observed down to 2.5, 3.8, and 1 kN−m for tests A, B, and C, respectively. As unloading continued, the wall moment remained relatively stable until an H/D ratio of approximately 2 was reached; at grain depths below this point, the wall moments decreased rapidly. This decrease in the wall moment was associated with the change in flow regime from mass flow to funnel flow. The wall moments then stabilized at an H/D ratio of 1.6, when a stable central flow channel within the bin was formed.

Wall Moments for Different Height of Attachment of Insert

Figure 6 shows the wall moments for the bin with no insert (test A) and the moments with a 23 cm wide insert spanning a 90˚ arc at H/D ratios of 0.95 (test B), 0.62 (test C), and 0.31 (test D). The insert was located in the (+*x*, −*y*) quadrant of the bin. For tests B, C, and D, the loading curves behaved similarly to that of a bin with no insert (test A) until the grain reached the attachment point of the insert. At this point, additional grain weight was transmitted to the wall because of the insert. Above this point, the insert counteracted the moment caused by imperfect centric filling. However, the filling curves were not identical for the three H/D ratios investigated.

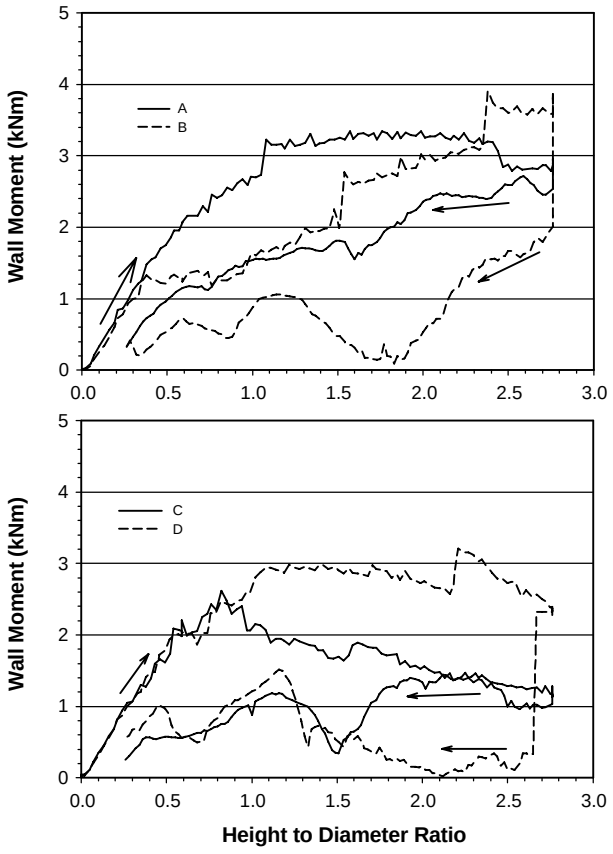

Figure 6. Wall moments produced during filling (arrows pointing to the right) and discharge (arrows pointing to the left) of the bin, with no insert (test A) and with a 90˚, 23 cm wide insert attached at H/D ratios of 0.95 (test B), 0.62 (test C), and 0.31 (test D).

Test B (insert located at an H/D ratio of 0.95) had a reduced wall moment of approximately 0.5 kN−m compared to test A (no insert). At an H/D ratio of 2.2, test B followed test A closely until the bin was full. The initiation of discharge resulted in a decrease in the wall moment that was particularly large for test B, where the wall moment decreased from 2.3 kN−m down to 0.4 kN−m. This was a result of initiation of mass flow, with grain moving down the wall and exerting a high vertical pressure on the insert. In this bin, the intersection of the flow channel with the bin wall during mass flow was observed at approximately 1.8 m (H/D = 0.74; Molenda et al., 2001).

Test C (insert located at an H/D ratio of 0.62) reached a maximum wall moment of 2.6 kN−m at an H/D ratio of approximately 0.8. As the fill height of the bin increased, the wall moment decreased to 1.1 kN−m at the end of filling. During discharge, the wall moment increased slightly until reaching an H/D ratio of approximately 1.7, when it decreased rapidly to a value less than 0.5 kN−m at an H/D ratio of 1.5. The wall moment then increased to approximately 1.0 kN−m and remained at that level until reaching an H/D ratio of 1.0, where it decreased until the bin was empty.

Test D (insert located at an H/D ratio of 0.31) followed the same path as the other tests until reaching an H/D ratio of 0.4. Between an H/D ratio of 0.4 and 1.5, the wall moment remained approximately 1.0 kN−m lower than in the other tests. At an H/D ratio of 1.5, the wall moment increased rapidly to a value of 2.75 kN−m, similar in magnitude to the values observed in tests A and B. At an H/D ratio of 2.3, the wall moment increased rapidly to a value of approximately 4 kN−m and then stabilized at a value of 3.5 kN−m until the bin was full. This increase in resultant wall moment for test D was mainly a result of an increase in the M_y component, which was distinctly higher than the value observed for test C. At the start of discharge, the wall moment decreased rapidly to a value of 2 kN−m. As the bin was emptied, the wall moment decreased until reaching an H/D ratio of 1.8, when the wall moment was approximately 0 kN−m. At an H/D ratio of 1.5, the wall moment increased to 1 kN−m until reaching an H/D ratio of 1.0, and then gradually decreased to zero.

At the start of discharge, the inserts located at H/D ratios of 0.62 and 0.31 (tests C and D) were immersed in a zone of stagnant grain where stress conditions did not change considerably. After the grain level decreased below an H/D ratio of 1.7, the flow pattern changed from mass flow to funnel flow, and the patterns of the moments in each test were similar.

Wall Moments for Different Insert Widths

Figure 7 shows the wall moments for inserts 7.6, 15, and 23 cm wide, spanning a 90˚ arc and attached to the bin wall at an H/D ratio of 0.62. The inserts were located in the (+*x*, +*y*) quadrant of the bin. During filling, the three curves followed a similar path up to an H/D ratio of 0.8. At this point, a wall moment of 2.2 kN−m was measured. Above this point, the grain depth for test A increased to a maximum value of 3 kN−m at an H/D of 1.3. During continued filling, the wall moments decreased to 2.5 kN−m at the end of filling. At the initiation of discharge, the wall moment decreased rapidly to a value of 1 kN−m. The moment then increased to approximately 2 kN−m at an H/D ratio of 2.0. At this point, the moment decreased rapidly to 0.7 kN−m at an H/D ratio of 1.5, increased slightly to 1.1 kN−m at an H/D ratio of 1.0, and then decreased during further unloading.

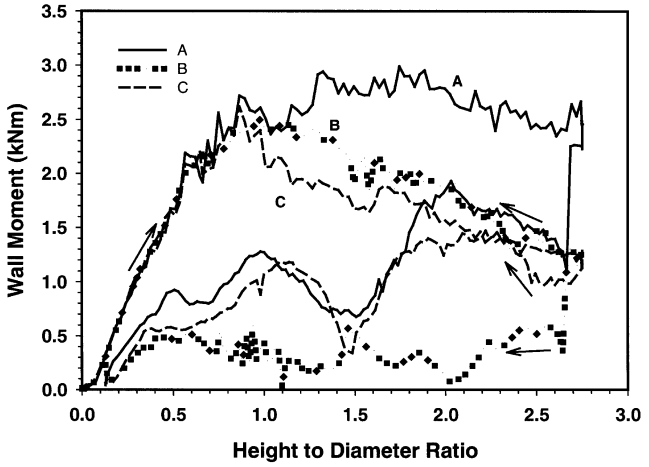

Figure 7. Wall moments produced during filling (arrows pointing to the right) and discharge (arrows pointing to the left) of the bin with 7.6 (test A), 15 (test B), and 23 cm (test C) wide, 90˚ inserts attached to the wall at H/D = 0.62.

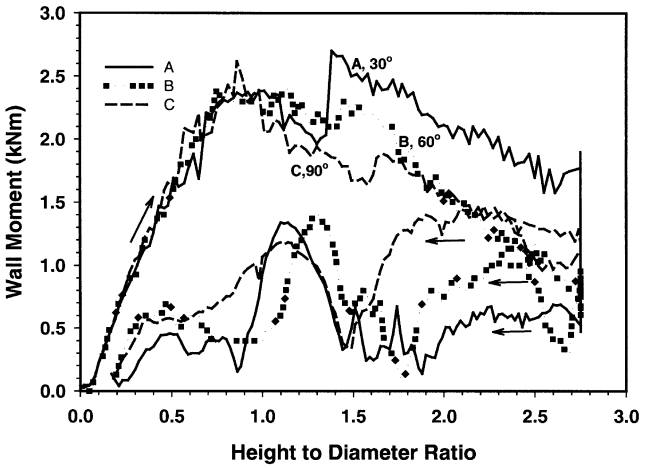

Figure 8. Wall moments produced during filling (arrows pointing to the right) and discharge (arrows pointing to the left) of the bin with a 23 cm wide insert with an angular extent of 30˚ (test A), 60˚ (test B), and 90˚ (test C) attached to the wall at H/D = 0.62.

The wall moment for test A was similar to the value for the bin with no insert (approximately 0.25 kN−m lower). The influence of the insert was more pronounced in tests B and C. After an H/D ratio of 0.85, the wall moments decreased to a value of 1.3 kN−m at the end of filling. At the start of discharge, the wall moment for test B decreased to 0.5 kN−m and did not exceed that value during discharge. Test C followed a similar path to test A but lagged the wall moments generated during test A by approximately 0.5 kN−m. Figure 7 demonstrates that wall moments were not proportional to the surface area of the inserts. Other factors influenced the vertical forces in the bins that were not quantifiable.

Wall Moments for Different Circular Extent of Insert

Figure 8 shows the wall moments during centric loading and discharge of the bin equipped with a 23 cm wide insert that spanned arcs of 30˚, 60˚, and 90˚, attached to the bin wall at an H/D ratio of 0.62 on the positive side of the *y* axis. The three curves followed a similar path during filling until the grain height reached an H/D ratio of 0.85, at which point the wall moment was 2.5 kN−m. Above this height, the influence of the insert was observed. For a bin with no insert (fig. 3), the wall moment increased during filling up to a value of 3.3 kN−m. However, with tests A, B, and C (fig. 8), the wall moments did not increase beyond 2.7 kN−m. The smallest insert created the largest wall moment during filling (test A). As the inserts increased in circumferential extent, the wall moments decreased. The inserts resulted in wall moments of 2.9, 1.7, 1.3, and 0.8 kN−m at the end of filling for no insert and tests A, B, and C, respectively.

During discharge, the sharpest decrease in the wall moment was observed for the smallest insert (test A). After a short period of fluctuations when mass flow developed, the wall moments increased for all tests. The moment for test A remained relatively constant at 0.55 kN−m until an H/D ratio of 2.0, when the moment began to fluctuate until an H/D ratio of 1.5. At that point, the moment increased to 1.3 kN−m at an H/D ratio of 1.2 and decreased below 0.5 kN−m for the remainder of discharge. Test B behaved similarly to test A, except the wall moment was approximately 0.4 kN−m larger at a grain height above an H/D ratio of 1.5.

During mass flow (until H/D of approximately 1.8), the wall moment was highest for test C and lowest for test A, with local maxima of 1.5 kN−m and 0.7 kN−m, respectively. Following this phase, the discharge pattern changed to funnel flow, which resulted in fluctuations in the resultant wall moments until the grain height passed an H/D ratio of approximately 1.2, after which the wall moment decreased continuously until the end of discharge. Figure 8 confirms the tendency that larger inserts had a stronger effect on the wall moment during loading and discharge.

Summary and Conclusions

A number of conclusions can be drawn from this study. Inserts on the grain bin wall resulted in an increased vertical wall load. The ratio of static vertical wall load to total grain load after the detention period was found in the range from 52% with no insert to 57% when an insert was attached to the wall with an arc length of 90˚, a width of 23 cm, and an H/D of 0.62. After 65 s of discharge, the ratio of vertical wall load to total grain load was found to vary from 60% to 64%. Values of dynamic−to−static wall load ratios were measured in the range from 1.11 to 1.16, without a clear relationship to the height or width of the insert.

It is normally assumed that centric filling results in a symmetric loading condition after filling. However, imperfect centric filling and non−uniformity of friction on the bin wall surface generated by the presence of the insert on the wall produced asymmetry of static wall loads after filling. The maximum wall moment observed after centric filling was found to be approximately 3 kN−m. Wall moments originating from the influence of the insert and imperfect centric filling together were determined using vector summation. For the worst−case condition, the total wall moment produced by a combination from both sources was 5 kN−m. In comparison, the maximum moment measured in the same bin during eccentric unloading (Molenda et al., 2001) was 13.1 kN−m. This level of global wall moment is not dangerous to the overall structure, but local stresses and deformation that cause such an asymmetry can result in the failure of the shell. The problem requires further examination with determination of local pressures.

The ratio of the vertical wall load with an insert to the vertical wall load with no insert was observed to stabilize during filling after the grain reached an H/D ratio of approximately 0.3 and remained steady until the end of filling. When discharge was initiated, the moments fluctuated and stabilized until the grain level reached an H/D ratio of 0.3. In the case of the largest insert (8.6% of the floor area), the ratio was observed in a range from 1.05 to 1.08. No clear difference was observed between different heights of attachment of the insert. In the case of the smallest inserts, their influence on loads was comparable to natural fluctuation of loads originating from non−homogeneity of the material and non−continuity of flow. Load fluctuations were higher during filling than during discharge because, in the latter case, the state of stress is closer to symmetric and the wall friction being mobilized is better defined. During filling, frictional forces of individual grains against the wall may take values in a range from minus maximum to plus maximum; thus, the resultant pressure is not as clearly defined. The extent to which wall friction develops depends on the shear displacement between the fill and the wall.

Acknowledgements

The authors wish to express their appreciation to the College of Agriculture, University of Kentucky, for sponsoring Dr. Molenda's visit to the Department of Biosystems and Agricultural Engineering, which made the research reported in this article possible. The part of the research performed in Poland was supported by the Polish Committee of Scientific Research under Grant No. 5 PO6F 021 17. This article is published with the approval of the Director of the Kentucky Agricultural Experiment Station and designated Paper No. 03−05−115.

References

Australian Standard AS 3774. 1996. Loads on bulk solids containers. Homebush, NSW: Standards Association of Australia.

Bucklin, R., S. A. Thompson, and I. J. Ross. 1990. Bin−wall failure caused by eccentric discharge of free−flowing grain. *J. Structural Eng.* 116(11): 3175−3190.

Carson, J. W. 2000. Silo failures: Case histories and lessons to learn. In *Proc. 3rd Israeli Conference for Conveying and Handling of Particulate Solids* 1: 4.1−4.11. Beer−Sheva, Israel: Ben−Gurion University of the Negev, Department of Mechanical Engineering.

CEN. 1996. Eurocode 1: Basis of design and actions on structures. Part 4: Actions on silos and tanks. ENV 1991−4. Brussels, Belgium: CEN.

Janssen, H. A. 1895. Versuche uber Getreidedruck in Silozellen. *Z. Ver. Dtsch. Ing.* 39: 1045−1049.

ISO. 1995. ISO 11697: Bases for design of structures − Loads due to bulk materials. Geneva, Switzerland: ISO.

Ketchum, M. S. 1919. *The Design of Walls, Bins, and Grain Elevators.* 3rd ed. New York, N.Y.: McGraw−Hill.

Molenda, M., J. Horabik, and I. J. Ross. 2001. Comparison of loads on smooth− and corrugated−wall model grain bins. *International Agrophysics* 15(2): 95−100.

Molenda, M., J. Horabik, I. J. Ross, and M. D. Montross. 2002. Friction of wheat: Grain−on−grain and on corrugated steel. *Trans. ASAE* 45(2): 415−420.

Ravenet, J. 1981. Silo problems. *Bulk Solids Handling* (1)4: 667−679.

Rotter, J. M. 1998. Shell structures: The new European standard and current research needs. *Thin−Walled Structures* 31(1−3): 3−23.

Sundaresan, S. 2001. Some outstanding questions in handling of cohesionless particles. *Powder Technology* 115(1): 2−7.

Timoshenko, S. 1910. Eiginge stabilitatsprobleme der elastizitats−theorie.*Zeitschrift fur Mathematik und Physik* 58(4): 337−385.

Tsunakawa, H., and R. Aoki. 1975. The vertical force of bulk solids on objects in bins. *Powder Technology* 11(3): 237−243.

Turitzin, A. M. 1963. Dynamic pressure of granular material in deep bins. *J. Structural Division ASCE* 89(ST2): 49−60.

Wilms, H.: 1994. Silo design for flow and strength: State−of−the−art and research requirements. *Powder Technology* (6)2: 193−196.